Progress In Electromagnetics Research, PIER 46, 313–333, 2004

INHOMOGENEOUS MAGNETIC MEDIA: WAVE PROPAGATION AND MAGNETIC PERMEABILITY RECONSTRUCTION

K. Baganás

Department of Materials Science and Engineering
University of Ioannina
GR45110 Ioannina, Greece

Abstract—In this paper we study the electromagnetic (EM) wave propagation in a perfect magnetic medium with continuously varying magnetic permeability $m(z)$ in one direction. We consider the inhomogeneity to be arbitrary and described by an infinite power series of z and use the Frobenious method to solve the governing differential equation of the problem in the frequency domain. We also give special attention to the first cut-off frequency of the main mode TM_{11} and we propose a good estimation for it by means of the mean value of the magnetic permeability profile. The results from the mathematical analysis are applied to solve the direct problem of wave propagation in a system of three waveguides having two homogeneous filling materials and one that exhibits such inhomogeneous characteristics. We finally confront the inverse problem of magnetic permeability reconstruction by handling simulation data and a genetic optimization algorithm.

1 Introduction

2 Maxwell's Equations in Inhomogeneous Media

3 Wave Propagation in a Rectangular Waveguide

4 The Direct Problem for a System of Rectangular Waveguides

4.1 Computation of the Field Components

4.2 Agreement with Existing Solutions

4.3 Cut-Off Frequencies

5 Solving the Inverse Problem

6 Numerical Results
6.1 Experiment Setup
6.2 Amplitude & Phase Parts Measurement
7 Conclusions
References

1. INTRODUCTION

The knowledge of the magnetic susceptibility and its spatial variations are of great importance in several applied scientific areas. For instance, in modeling electromagnetic fields in geophysical explorations, there are many practical situations when a conductive object has significant magnetic properties. For example, a magnetite-containing ore body and drilling mud with heavy material ingredients are characterized by both a strong anomalous conductivity and a magnetic susceptibility, which can produce significant effects on the electromagnetic tool response. In geoelectrical exploration, the magnetic properties of rocks and especially their anomalous behavior are of crucial interest as well. Magnetic susceptibility information is also important in many areas of bioengineering, medical applications and telecommunications.

Various methods have been applied so far for the determination or simply the estimation of the unknown varying magnetic properties of media of interest. For example, in geoelectrical exploration the so-called S_μ method [1–3] add the possibility to recover the magnetic properties of geological bodies and to reconstruct both anomalous conductivity and magnetic permeability characteristics from the same time domain magnetic field data. Cheryauka and Zhdanov [4] extend linear and nonlinear approximations for electromagnetic fields in a medium with inhomogeneous distribution of both electrical and magnetic material properties. These approximations form a basis for fast EM modeling and imaging in multi-dimensional environments where joint electrical and magnetic inhomogeneity is an essential feature of the model. In metallic thin films technology the determination of the composition of thin films with high resolution in the nanometer region is necessary. For this purpose, the so called mixing-roughness-information depth (MRI)-model is developed for profile reconstruction and quantification. Also, in bioengineering various theories have been developed for true 3D susceptibility mapping in general situations of arbitrary susceptibility distributions.

Realistic computational models of inhomogeneous dielectric and/or magnetic media considered in applications, such as wave scattering by arbitrary shaped inhomogeneous obstacles and wave propagation in stratified media in telecommunications, engineering and in geological exploration, are based most on approximate numerical methods; i.e., finite elements, finite differences, boundary integral equations and spectral methods. Analytical methods, of course, cannot handle such demanding applications, but are good candidates to apply in certain cases where the geometries of the applications are similar to coordinate surfaces (e.g., rectangular, cylindrical or spherical), the domains occupied by the inhomogeneities have also characteristic shapes and the varying material properties are piecewise smooth. In literature, analytical treatments of piecewise constant, linear and quadrature inhomogeneities can easily be found; especially, in elastic and dielectric inhomogeneous media. The luck of similar studies in magnetic media is a surprising fact since various scientific disciplines meet such materials and the reciprocal theorems encountered in many applied fields (e.g., in Maxwell's equations) provide a straightforward way to apply in inhomogeneous magnetic materials.

Having in mind the statement above, we suggest, in this paper, a simplified theoretical model for a non-destructive testing setup, consisted of three rectangular waveguides, which can be applied to estimate the unknown magnetic permeability profile of a material. The present analysis follows the methodology in [5] and [6] and can be applied to all inhomogeneous magnetic profiles of the form $\mu(z) = \mu^*\mu_r(z)$, where μ^* is the magnetic permeability in free space and $\mu_r(z)$ denotes the relative magnetic permeability. The only requirement for $\mu_r(z)$ is to be continuous so as expansion in *power series* of z is valid.

Briefly, we study Maxwell's equations for such media by applying separation of variables in rectangular coordinates. Taking advantage of the polynomial form of $\mu_r(z)$ we use the *Frobenius* method and we conclude for the z-dependent part of the electric field, in an ODE with nonconstant coefficients. Then, the recursive equations for the expansion coefficients of the electric field, that arise, can be solved symbolically or numerically. The results taken from this mathematical analysis are used to solve the direct problem for the wave propagation in the system of waveguides. The central one has an inhomogeneous magnetic filling and the two lateral ones are filled up with homogeneous materials. Then we proceed in the magnetic profile reconstruction which constitutes the inverse problem. We utilize an error function minimization approach which makes use of a genetic algorithm and seeks for the unknown coefficients μ_0, μ_1, μ_2... in the $\mu_r(z)$ expansion. Note, that we solve the inverse problem for the case of cubic inhomogeneity, which is quite sufficient for many real-world applications. Finally, we give some representative numerical results that verify the applicability of our reconstruction approach.

2. MAXWELL'S EQUATIONS IN INHOMOGENEOUS MEDIA

Considering a longitudinally inhomogeneous, magnetic material with magnetic permeability $\mu(z) = \mu^* \mu_r(z)$, Maxwell's equations yield the following equations, which characterize the phasor $\mathbf{H}(\mathbf{r})$ of the time harmonic magnetic field

$$\nabla \cdot (\mu_r(z)\mathbf{H}) = 0 \tag{1}$$

$$\nabla(\nabla \cdot \mathbf{H}) - \nabla^2 \mathbf{H} = k^2 \mu_r(z)\mathbf{H} \tag{2}$$

where $k = \omega\sqrt{\mu^*\epsilon^*}$ is the wavenumber, while $\omega = 2\pi f$ is the angular frequency and μ^*, ϵ^* are the magnetic permeability and the electric permittivity in free space, correspondingly.

We are interested in TM modes which are expressed in rectangular coordinates x, y, z by the form

$$\mathbf{H}(r, \phi, z) = H_x(x,\, y,\, z)\hat{\mathbf{x}} + H_y(x,\, y,\, z)\hat{\mathbf{y}} \tag{3}$$

where $\hat{\mathbf{x}}$, $\hat{\mathbf{y}}$ are the unit vectors. Applying separation of variables, the components of the electric field become

$$H_x(x,y,z) = X_x(x)\, Y_x(y)\, Z_x(z)\ , \quad H_y(x,y,z) = X_y(x)\, Y_y(y)\, Z_y(z)\,.$$

Inserting these expressions in Eq. (1), we obtain

$$\frac{X_x'}{X_x} + \frac{X_y}{X_x}\frac{Y_y'}{Y_x}\frac{Z_y}{Z_x} = 0$$

or equivalently

$$Z_y = \kappa Z_x\ , \tag{4}$$

$$Y_y' = \lambda Y_x\ , \tag{5}$$

$$X_x' = -\kappa\lambda X_y\ , \tag{6}$$

where κ, λ are constant coefficients.

Moreover Eq. (2), in accordance with Eq. (4) and after submission to separation of variables treatment gives birth to the following scalar differential equations

$$\frac{X_x''}{X_x} + \frac{Y_x''}{Y_x} + \frac{Z_x''}{Z_x} + k^2\mu_r(z) = 0\ , \tag{7}$$

$$\frac{X_y''}{X_y} + \frac{Y_y''}{Y_y} + \frac{Z_y''}{Z_y} + k^2 \mu_r(z) = 0\,. \tag{8}$$

Handling Eq. (7) first, we apply standard separation of variable arguments leading to the relations

$$\frac{X_x''}{X_x} = -p^2\ , \quad (p \text{ constant}) \tag{9}$$

$$\frac{Y_x''}{Y_x} = -q^2\ , \quad (q \text{ constant}) \tag{10}$$

$$Z_x'' + \left[k^2 \mu_r\,(z) - \xi^2\right] Z_x = 0\ , \tag{11}$$

where $\xi^2 = p^2 + q^2$. The general solutions of Eqs. (9), (10) are

$$X_x(x) = A_1 \cos(px) + A_2 \sin(px) \tag{12}$$

and

$$Y_x(y) = B_1 \cos(qy) + B_2 \sin(qy) \tag{13}$$

when $p, q \neq 0$ and A_1, A_2, B_1, B_2 are arbitrary constants. The case $p = 0$ or/and $q = 0$ will be analyzed later.

Special treatment is needed for Eq. (11) to obtain its general solution. The relative magnetic permeability has a power series expansion of the form

$$\mu_r(z) = \sum_{i=0}^{\infty} \mu_i z^i = \mu_0 + \mu_1 z + \mu_2 z^2 + \dots\,. \tag{14}$$

We use Frobenius method for solving Eq. (11) and assume that $Z_x(z)$, the solution to this equation, can be expressed as

$$Z_x(z) = \sum_{i=0}^{\infty} c_i z^i = c_0 + c_1 z + c_2 z^2 + \dots \tag{15}$$

given that the center of expansion 0 is a regular point for the ODE (11). Hence $Z_x(z)$ is determined by the coefficients c_i, $i = 0, 1, 2, \dots$. From now on our analysis will focus on determining these coefficients.

Substituting the expressions (14), (15) in Eq. (11) and equating the coefficients of the powers of coordinate z, we produce the following recursive scheme

$$(i+2)(i+1)c_{i+2} - \xi^2 c_i + k^2 \sum_{j=0}^{i} c_{i-j}\mu_j = 0\ , \quad i = 0, 1, 2, \dots\,.$$

Equivalently, setting $H^2 = k^2\mu_0 - \xi^2$ we have

$$c_2 = -\frac{H^2}{2}c_0 \text{ and } (i+2)(i+1)c_{i+2}+H^2c_i+k^2\sum_{j=1}^{i} c_{i-j}\mu_j = 0,\ i = 1, 2, \ldots . \tag{16}$$

From this scheme we infer that c_i $(i \geq 2)$ are functions of c_0, c_1, H, k and the permittivity coefficients μ_j, $j = 0,..,i-2$, i.e., $c_i = c_i(c_0,\, c_1,\, H,\, k,\, \mu_0, .., \mu_{i-2})$. More accurately, c_i can be written as:

$$c_i = c_0 u_i(H,\, k,\, \mu_0, .., \mu_{i-2})\ +\ c_1 w_i(H,\, k,\, \mu_0, .., \mu_{i-2})$$

where u_i, w_i are smooth functions of their arguments. For example, for $i = 1$ in Eq. (16), we obtain $c_3 = -\frac{H^2}{6}c_1 - \frac{k^2}{6}\mu_1 c_0$, where $u_3(\cdot) = -\frac{H^2}{6}$ and $w_3(\cdot) = -\frac{k^2}{6}\mu_1$. Also, for $i = 2$ we obtain $c_4 = (\frac{H^4}{2} - k^2\mu_2)\frac{C_0}{12} - \frac{k^2\mu_1}{12}c_1$, where $u_4(\cdot) = (\frac{H^4}{2} - k^2\mu_2)\frac{1}{12}$ and $w_4(\cdot) = -\frac{k^2\mu_1}{12}$.

Combining the expressions (12), (13) and (15) we obtain the general form of the x-component of the magnetic field:

$$\begin{aligned} H_x(x, y, z) \ &=\ [A_1\cos(px) + A_2\sin(px)]\cdot[B_1\cos(qy) + B_2\sin(qy)] \\ &\quad \cdot\left(\sum_{i=0}^{\infty} c_i z^i\right) \end{aligned} \tag{17}$$

Handling now Eq. (8) with the same manner we obtain an analogous expression for the y-component of the magnetic field:

$$\begin{aligned} H_y(x, y, z) \ &=\ [C_1\cos(px) + C_2\sin(px)]\cdot[D_1\cos(qy) + D_2\sin(qy)] \\ &\quad \cdot k\left(\sum_{i=0}^{\infty} c_i z^i\right) \end{aligned} \tag{18}$$

where p, q, c_i are the same coefficients as in the Eq. (17) (this can be explained through consideration of Eqs. (4), (5), (6)) and C_1, C_2, D_1, D_2 are arbitrary constants. Remark that the multiplicative scalar k has been added in order for Eq. (4) to be satisfied.

Once the recursive Equations (16) are solved, the sought "axial" parts $Z_x\,(z)$, $Z_y\,(z)$ of the magnetic fields are determined through their power series coefficients. All the other components of the fields have been already determined and so the solution of the Equations (16) leads immediately to the solution of Maxwell's equations for the specific structure under consideration. The behavior of c_2, c_3, .., c_L can be studied analytically for small values of L; larger values of L require the use of a symbolic algebra package, e.g. *Maple.*

Full consideration of Eqs. (4), (5), (6), or equivalently satisfaction of Eq. (1) demand that the mixture coefficients do not be independent, but satisfy the following equations

$$C_1 = -\frac{A_2 p}{\kappa\lambda}\,, \quad C_2 = \frac{A_1 p}{\kappa\lambda}\,, \tag{19}$$

$$D_1 = -\lambda\frac{B_2}{q}\,, \quad D_2 = \lambda\frac{B_1}{q} \tag{20}$$

Consequently, the final solutions are

$$H_x(x,y,z) = [A_1\cos(px) + A_2\sin(px)] \cdot[B_1\cos(qy) + B_2\sin(qy)]\cdot\left(\sum_{i=0}^{\infty} c_i z^i\right)\,, \tag{21}$$

$$H_y(x,y,z) = \frac{p}{q}[A_1\sin(px) - A_2\cos(px)] \cdot[B_1\sin(qy) - B_2\cos(qy)]\cdot\left(\sum_{i=0}^{\infty} c_i z^i\right)\,. \tag{22}$$

Any arbitrary coefficients appearing in the above solutions will be specified by boundary independent conditions pertaining to a specific problem.

Before proceeding further, let us mention that there exist three special cases concerning the values of the separation of variables constants p and q not discussed before.

1. When $p = 0$ and $q \neq 0$, the x-components X_x, X_y becomes: $X_x(x)A_1x + A_2$ and $X_y(x) = C_1x + C_2$. Insertion of these expressions in Eq. (6) and the combination of the results of Eqs. (4), (5) leads to the elimination of the C_1 coefficient and to the general solutions which are

$$H_x = (A_1x + A_2)\cdot[B_1\cos(qy) + B_2\sin(qy)]\cdot\left(\sum_{i=0}^{\infty} c_i z^i\right), \tag{23}$$

$$H_y = \frac{A_1}{q}\cdot[B_2\cos(qy) - B_1\sin(qy)]\cdot\left(\sum_{i=0}^{\infty} c_i z^i\right), \tag{24}$$

2. When $q = 0$ and $p \neq 0$, analogous treatment leads to the following general solutions

$$H_x = \frac{D_1}{p}\cdot[C_2\cos(px) - C_1\sin(px)]\cdot\left(\sum_{i=0}^{\infty} c_i z^i\right)\,, \tag{25}$$

$$H_y = [C_1 \cos(px) + C_2 \sin(px)] \cdot (D_1 y + D_2) \cdot \left(\sum_{i=0}^{\infty} c_i z^i \right) . \quad (26)$$

3. When $p = 0$ and $q = 0$, the general solutions are

$$H_x = (A_1 x + A_2) \cdot \left(\sum_{i=0}^{\infty} c_i z^i \right) , \quad (27)$$

$$H_y = (-A_1 y + D_2) \cdot \left(\sum_{i=0}^{\infty} c_i z^i \right) . \quad (28)$$

3. WAVE PROPAGATION IN A RECTANGULAR WAVEGUIDE

We now exploit the appropriate boundary conditions regarding the field solutions in the previous section.

The remarks and expressions presented below apply to the case of $\mu(x, y, z) = \mu^* \mu_r(z)$, as well as to the special case of constant magnetic permeability. The following conditions must be satisfied by the TM magnetic field.

Condition 1: The magnetic field components must have bounded values inside the waveguide.

Condition 2: The normal component must vanish on the surface of the waveguide (i.e., at $x = 0, a$ and $y = 0, b$, where a is the width and b is the height of the cross-section of the waveguide).

Let us examine the general solution for all the cases of p, q in light of the above conditions.

Condition 1 is immediately satisfied for all values of p, q. Condition 2 leads to the above cases.

Case 1: $p, q \neq 0$: Condition 2 implies that $A_1 = B_2 = 0$ and leads to the discretization of p, q; i.e., $p = p_m = \frac{m\pi}{a}$ and $q = q_n = \frac{n\pi}{b}$, where $w, n = 1, 2, \ldots$. So, the expressions of the TM_{mn} modes are

$$H_x(x, y, z) = H_0 \sin(p_m x) \cos(q_n y) \cdot (\sum_{i=0}^{\infty} c_i z^i) , \quad (29)$$

$$H_y(x, y, z) = -\frac{p_m}{q_n} H_0 \cos(p_m x) \sin(q_n y) \cdot (\sum_{i=0}^{\infty} c_i z^i) , \quad (30)$$

where H_0 is an arbitrary amplitude.

Case 2: $p \neq 0$, $q = 0$: Condition 2 implies that $D_1 = D_2 = 0$ and TM_{m0} modes are vanished.

Case 3: $p = 0$, $q \neq 0$: Condition 2 implies that $E_0 = 0$ and TM_{0n} modes are vanished too.

Case 4: $p = q = 0$: Condition 2 implies that TM_{00} are vanished.

It is clear that only TM_{mn} $(m, n \neq 0)$ modes propagate along a rectangular waveguide fulfilled with an inhomogeneous magnetic material.

4. THE DIRECT PROBLEM FOR A SYSTEM OF RECTANGULAR WAVEGUIDES

In order to solve the direct problem we utilize a *measurement device* consisted of three rectangular waveguides interconnected as Figure 1 illustrates.

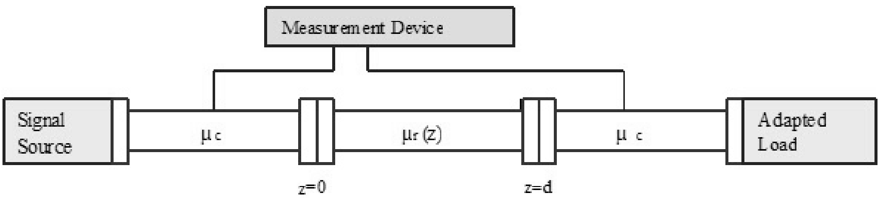

Figure 1. The measurement device.

The left and the right waveguide have fillings with constant relative magnetic permeability μ_c. The middle one contains an inhomogeneous magnetic filling. This will be the target of our investigation of the inverse problem. The waveguides are being excited by appropriate TM electric modes generated by the signal source. We consider perfect interconnections among the waveguides and a load adapted to the end of the right waveguide. These assumptions result in non-dissipative wave propagation and perfect/ideal absorption of the incident wave at the load.

We study the propagation of the TM_{11} mode, which is the main mode for rectangular waveguides, and we assume a third order polynomial expansion for the permeability $\mu_r(z)$ i.e.,

$$\mu_r(z) = \mu_0 + \mu_1 z + \mu_2 z^2 + \mu_3 z^3 .$$

4.1. Computation of the Field Components

We handle first the frequencies at which field propagation occurs.

The cut-off frequencies for the two lateral waveguides, which have relative permeability $\mu_r = \mu_c$, are the following [7]

$$\mathbf{f}_{c,mn} = \frac{1}{2\pi}\sqrt{\frac{\left(\frac{m\pi}{a}\right)^2 + \left(\frac{n\pi}{b}\right)^2}{\mu^*\epsilon^*\mu_c}}\,, \quad m,\, n = 0, 1, 2, \dots. \tag{31}$$

This implies that the excitation frequency f must be greater than the first cut-off frequency $\mathbf{f}_{c,11}$ which is

$$\mathbf{f}_{c,11} = \frac{1}{2}\sqrt{\frac{\left(\frac{1}{a}\right)^2 + \left(\frac{1}{b}\right)^2}{\mu^*\epsilon^*\mu_c}}. \tag{32}$$

So, the use of excitation frequency $f > \mathbf{f}_{c,11}$ is a prerequisite for the transmission of a wave along the system of waveguides. In what follows μ_c is the constant relative permeability of the filling either in the left or the right waveguide, $\beta = \sqrt{k^2\mu_c - (\frac{\pi}{a})^2 - (\frac{\pi}{b})^2}$, $k = \omega\sqrt{\mu^*\epsilon^*}$.

Waveguide no.1: The field expression is

$$H_x(x,\, y,\, z) \;=\; H_0 \sin\left(\frac{\pi x}{a}\right)\cos\left(\frac{\pi y}{b}\right)\left(e^{-j\beta z} + Ge^{j\beta z}\right) \tag{33}$$

$$H_y(x,\, y,\, z) \;=\; -\frac{b}{a}H_0 \cos\left(\frac{\pi x}{a}\right)\sin\left(\frac{\pi y}{b}\right)\left(e^{-j\beta z} + Ge^{j\beta z}\right) \tag{34}$$

where H_0 is an arbitrary amplitude constant and G is the *reflection coefficient.*

Waveguide no.2: The field expression is

$$H_x(x,\, y,\, z) \;=\; H_0 \sin\left(\frac{\pi x}{a}\right)\cos\left(\frac{\pi y}{b}\right)\sum_{i=0}^{\infty} c_i z^i\,. \tag{35}$$

$$H_y(x,\, y,\, z) \;=\; -\frac{b}{a}H_0 \cos\left(\frac{\pi x}{a}\right)\sin\left(\frac{\pi y}{b}\right)\sum_{i=0}^{\infty} c_i z^i\,. \tag{36}$$

Waveguide no.3: The field expression is

$$H_x(x,\, y,\, z) \;=\; D\sin(\frac{\pi x}{a})\cos\left(\frac{\pi y}{b}\right)e^{-j\beta z}\,, \tag{37}$$

$$H_y(x,\, y,\, z) \;=\; -\frac{b}{a}D\cos\left(\frac{\pi x}{a}\right)\sin\left(\frac{\pi y}{b}\right)e^{-j\beta z}\,, \tag{38}$$

where D is the *transmission coefficient.*

We now set $\boldsymbol{\mu} = [\mu_0\ \mu_1\ \mu_2\ \mu_3]$. Recall that in the framework of the inverse problem the quantities obtained by the measurement device will be $D = D(\boldsymbol{\mu}, f, a, b, d)$, $G = G(\boldsymbol{\mu}, f, a, b, d)$, where f, a, b, d will be known for a particular experiment, while $\boldsymbol{\mu}$ will be the quantity we want to determine. In fact D, G can be measured; we will now determine their functional dependence on μ_0, μ_1, μ_2, μ_3 (and f, a, b, d); our final task will be to determine appropriate values for μ_0, μ_1, μ_2, μ_3 such that the theoretically computed D, G measurements agree with the ones obtained from field measurements.

Hence our next task is to obtain concrete functional expressions for $D(\boldsymbol{\mu}, f, a, b, d)$ and $G(\boldsymbol{\mu}, f, a, b, d)$. To this end we use the impedance conditions for the three waveguides.

At the interface $z = 0$, from the continuity of the components and their derivatives, we have that

$$c_0 = 1 + G \tag{39}$$

$$c_1 = -j\beta \cdot (1 - G)\,. \tag{40}$$

Similarly, at the interface $z = d$ the continuity of the components and their derivatives leads to

$$c_0 Z_1(d) + c_1 Z_2(d) = \frac{D}{H_0} e^{-j\beta d} \tag{41}$$

$$c_0 Z_1'(d) + c_1 Z_2'(d) = -j\beta \frac{D}{H_0} e^{-j\beta d} \tag{42}$$

where $Z_1(d) = 1 + u_2 d^2 + u_3 d^3 + \ldots$ and $Z_2(d) = d + w_2 d^2 + w_3 d^3 + \ldots$. Eqs.(39-42) can be written as a 4×4 linear system: $AX = B$, where

$$A = \begin{bmatrix} 1 & 0 & -1 & 0 \\ 0 & 1 & -j\beta & 0 \\ Z_1(d) & Z_2(d) & 0 & -e^{-j\beta d}/H_0 \\ Z_1'(d) & Z_2'(d) & 0 & j\beta e^{-j\beta d}/H_0 \end{bmatrix},$$

$$X = \begin{bmatrix} c_0 \\ c_1 \\ G \\ D \end{bmatrix}, \quad B = \begin{bmatrix} 1 \\ -j\beta \\ 0 \\ 0 \end{bmatrix}.$$

Hence A and B are completely specified in terms of known parameters, X contains the unknowns of the direct problem and $AX = B$ is a linear matrix equation which can be solved analytically by matrix inversion.

4.2. Agreement with Existing Solutions

We will now test the agreement of our solution with already existing analytical solutions for two simple magnetic profiles.

Case 1: $\mu_r(z) \equiv \mu_m =$ constant. In this case the field expressions inside the medium waveguide become

$$H_x(x, y, z) = H_0 \sin\left(\frac{\pi x}{a}\right)\cos\left(\frac{\pi y}{b}\right)\left(C_m e^{-j\beta_m z} + G_m e^{j\beta_m z}\right),$$

where m denotes the medium waveguide, C_m is the propagation coefficient, G_m is the reflection coefficient and $\beta_m = \sqrt{k^2\mu_w - \left(\frac{\pi}{a}\right)^2 - \left(\frac{\pi}{b}\right)^2}$. Applying the same boundary conditions between the waveguides we obtain the corresponding 4×4 linear system $AX = B$, where

$$A = \begin{bmatrix} 1 & 1 & -1 & 0 \\ \beta_m & -\beta_m & \beta & 0 \\ e^{-j\beta_m d} & e^{j\beta_m d} & 0 & -e^{-j\beta d}/H_0 \\ \beta_m e^{-j\beta_m d} & -\beta_m e^{j\beta_m d} & 0 & -\beta e^{-j\beta d}/H_0 \end{bmatrix},$$

$$X = \begin{bmatrix} C_m \\ G_m \\ G \\ D \end{bmatrix}, \quad B = \begin{bmatrix} 1 \\ \beta \\ 0 \\ 0 \end{bmatrix}.$$

We solve this system for various profiles μ_m, in an efficient range of frequencies in which our method converges, obtaining values for G, D which are in excellent agreement with our Frobenius approximations.

We would like herein to mention that the necessary condition for convergence: $\lim_{i\to\infty} |c_i z^i| = 0$ is satisfied for every $z \in [0, d]$ and for an adequate range of frequencies, as will be explained next. As an example, for $\mu_m = 50$ and for $z = 0.1 : |c_i z^i| \leq 10^{-16}$ for $i \geq 60$ at the frequency of 1.2 GHz. In addition, the rate of convergence is controlled by comparing the influence of additional terms in the partial Frobenius sum in every step; i.e., if $S_i = \sum_{n=0}^{i} c_n z^n$, then $\left|\frac{S_i - S_{i+j}}{S_i}\right| \leq 10^{-16}$ for $i \geq 60$. The rate of convergence varies as frequency changes. As the latter increases the rate decreases. For example, when $f = 1.5$ GHz then $\left|\frac{S_i - S_{i+j}}{S_i}\right| \leq 10^{-16}$ for $i \geq 77$ and every $j \geq 1$. Also, for the case of an arbitrary cubic inhomogeneous profile, say $\mu = [3000 \quad 185.47 \quad 200.24 \quad -2946.92]$, we obtain $\left|\frac{S_i - S_{i+j}}{S_i}\right| \leq 10^{-16}$ for $i \geq 57$ at the frequency of 150 MHz and $i \geq 116$ at the frequency of 300 MHz.

Generally speaking, in all cases of inhomogeneous profiles we have examined, 120 terms of $c_i z^i$ in the Frobenius series were quite sufficient to represent the solution accurately and in a stable manner.

Case 2: $\mu_r(z) = a + bz$. In the case of linear inhomogeneity Eq. (11) becomes

$$\begin{aligned} Z_y'' + [k^2(a+bz) - \xi^2] \cdot Z_y &= 0 \Leftrightarrow Z_y'' + (k^2 a - \xi^2 + k^2 bz) \cdot Z_y \\ &= 0 \Leftrightarrow Z_y'' + (A + Bz) \cdot Z_y = 0, \end{aligned}$$

where $A = k^2 a - \xi^2$ and $B = k^2 b$. Applying the change of independent variable: $n(z) = -B^{1/3} \cdot (z + \frac{A}{B})$, we obtain

$$\ddot{Z}_y = n Z_y \tag{43}$$

where $\ddot{Z}_y$ denotes the second derivative with respect to n. The general solution of (43) is a linear combination of the *Airy's* functions $Ai(n)$, $Bi(n)$, of the first and second kind, respectively. Consequently, the z-dependent part of the field component has the expression

$$Z_y(z) = a_1 Ai(n(z)) + a_2 Bi(n(z)) \,,$$

where a_1, a_2 are arbitrary coefficients. Therefore, the field inside the medium waveguide can be explicitly written as

$$H_x(x,\, y,\, z) = H_0 \sin\left(\frac{\pi x}{a}\right) \cos\left(\frac{\pi y}{b}\right) \cdot \left[a_1 Ai(n(z)) + a_2 Bi(n(z))\right].$$

Applying the same boundary conditions at the points $z = 0 \Leftrightarrow n_0 \equiv n(0) = -\frac{A}{B^{2/3}}$ and $z = d \Leftrightarrow n_d \equiv n(d) = -B^{-1/3} \cdot (d + \frac{A}{B})$ we obtain the corresponding 4×4 linear system $AX = B$, where

$$A = \begin{bmatrix} Ai(n_0) & Bi(n_0) & -1 & 0 \\ -B^{1/3} Ai'(n_0) & -B^{1/3} Bi'(n_0) & -j\beta & 0 \\ Ai(n_d) & Bi(n_d) & 0 & -e^{-j\beta d}/H_0 \\ -B^{1/3} Ai'(n_d) & -B^{1/3} Bi'(n_d) & 0 & j\beta e^{-j\beta d}/H_0 \end{bmatrix},$$

$$X = \begin{bmatrix} a_1 \\ a_2 \\ G \\ D \end{bmatrix}, \quad B = \begin{bmatrix} 1 \\ -j\beta \\ 0 \\ 0 \end{bmatrix}.$$

We solve this system numerically for various linear profiles $\mu_r(z) = a + bz$ and we obtain values for G and D which are also in an extremely close agreement with our Frobenius approximation. For example, in

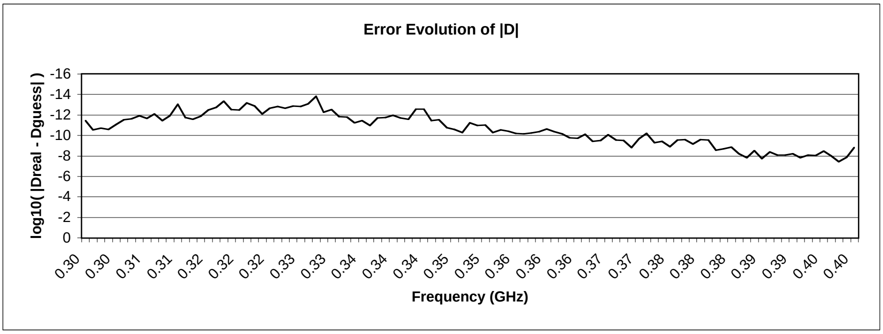

Figure 2. Error of the absolute value of D as a function of f, for the linearly varying magnetic profile $\mu_r(z) = 428 + 520,5z$. (Computed as the logarithm of the relative difference between our solution and the one involving Airy's functions.)

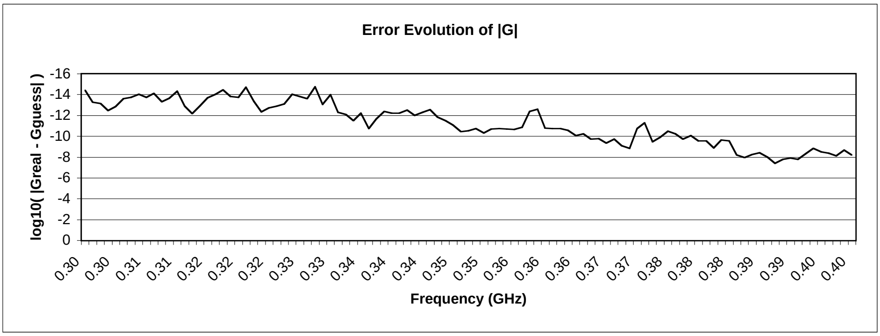

Figure 3. Error of the absolute value of G as a function of f, for the linearly varying magnetic profile $\mu_r(z) = 428 + 520,5z$. (Computed as the logarithm of the relative difference between our solution and the one involving Airy's functions.)

the case of an arbitrary linear profile, this agreement is verified in Figures 2 and 3 given below.

Hence our solutions (obtained using Frobenius method) are in agreement with independently obtained and well known solutions for the two types of profiles discussed above.

4.3. Cut-Off Frequencies

In the previous papers [5] and [6] we established relations concerning the first cut-off frequency of the main propagating mode and the mean value of the inhomogeneous dielectric profiles. According to what follows a similar relation holds for the inhomogeneous magnetic profiles as well.

Namely, a very good approximation for $\mathbf{f}_{c,11}$, can be given by utilizing a formula analogous to the one applying in the case of constant magnetic permeability; i.e.,

$$[\mathbf{f}]_{c,11} = \frac{1}{2}\sqrt{\frac{\left(\frac{1}{a}\right)^2 + \left(\frac{1}{b}\right)^2}{\mu^*\epsilon^*[\mu]}} \tag{44}$$

(where $[\mu] = \frac{1}{d}\int_0^d \mu_r(z)dz$ is the mean value of the magnetic profile). Hence, combining Eq. (44) with an experimental value of $\mathbf{f}_{c,11}$ we obtain an estimation for the mean value of an unknown inhomogeneity.

The next table presents the values of $\mathbf{f}_{c,11}$ and $[\mathbf{f}]_{c,11}$ for some representative magnetic profiles.

Table 1. A list of inhomogeneous profiles, their mean value $[\mu]$ and the corresponding real $f_{c,11}$ and approximate $[f]_{c,11}$ cut-off frequency.

$\mu_r(z)$	$[\mu]$	$f_{c,11}$ (GHz)	$[f]_{c,11}$ (GHz)
40 + 5.47z	40.547	1.05	1.08
290 — 185.7z	271.43	0.407	0.419
850 + 155.3z	865.53	0.228	0.278
1500 + 510.5z	1551.05	0.168	0.171
3000 + 300.3z	3030.03	0.127	0.122
5000 + 330.2z	5033.02	94.49(MHz)	94.425(MHz)
10000 — 590z	9941	67.23(MHz)	67.05(MHz)
40 + 5.47z — 90.24z^2	39.34	1.068	1.096
290 — 85.47z + 150.24z^2	283.46	0.398	0.4
850 + 55.3z — 520.24z^2	848.6	0.230	0.231
1500 + 210.5z — 840.24z^2	1509.8	0.173	0.173
3000 + 100.3z — 1200.4z^2	2994	0.123	0.122
5000 + 130.2z — 1350z^2	4995	94.85(MHz)	94.95(MHz)
10000 — 250z — 1170.4z^2	9959.4	67.17(MHz)	67(MHz)
30 — 4.7z + 8.24z^2— 130.92z^3	29.38	1.248	1.242
290 — 30.47z + 290.24z^2— 130.92z^3	290.63	0.393	0.396
850 — 13.47z + 290.24z^2— 96.92z^3	852.33	0.23	0.231
1500 — 200.47z + 150.24z^2— 2300.92z^3	1477.35	0.174	0.175
3000 + 185.47z + 200.24z^2 — 2946.92z^3	3015.32	0.122	0.123
5000 — 280.47z + 1200z^2— 8946.92z^3	4970	95.1(MHz)	95.25(MHz)
10000 — 250.47z + 1180.24z^2— 12300.92z^3	9966.1	67.15(MHz)	67.05(MHz)

The figure below provides a better inspection of Table 1's data.

Note that for only one of twenty one profiles the error approaches 20%; for the rest ones remains strictly less than 3%. This means that $[\mathbf{f}]_{c,11}$ is very possible to be a quite accurate approximation.

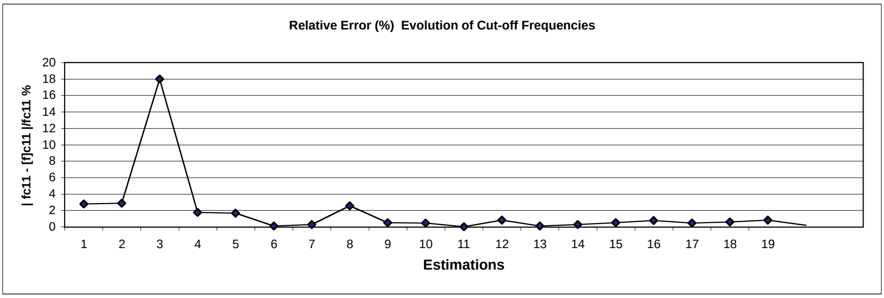

Figure 4. Relative error (%) between $f_{c,11}$ (real) and $[f]_{c,11}$ corresponding to twenty one (21) arbitrary chosen inhomogeneous magnetic profiles.

5. SOLVING THE INVERSE PROBLEM

We follow exactly the same approach as in [5]. Briefly, handling the *simulation's experiment* data we form a *function minimization* procedure using a *genetic Differential Evolution (DE) optimization algorithm* [8].

6. NUMERICAL RESULTS

We now present the results of our *simulated experiments*. We postulate a three-waveguide measurement system of the form presented in Section 4.1 with $d = 20\,\text{cm}$, $a = 2.5\,\text{cm}$, $b = 5\,\text{cm}$ and specific $\boldsymbol{\mu}^i = [\mu_0^i\ \mu_1^i\ \mu_2^i\ \mu_3^i]$ and μ_c values, where i represents the i profile under consideration. Then we obtain numerical values for the field in the system by utilizing the analysis presented in Section 4.1. These numerical values are our "virtual measurements". Then, we assume the $\boldsymbol{\mu}^i$ values to be unknown and we utilize the error function minimization formulation and the inverse problem solution of Section 5 to obtain "good" estimates $\widehat{\boldsymbol{\mu}^i}$ for the real $\boldsymbol{\mu}^i$ values (i.e., estimates $\widehat{\boldsymbol{\mu}^i}$ which yield a near zero value for the error function).

We also give arbitrary values for the permittivity μ_c; i.e., $\mu_c^1 = 5000$ and $\mu_c^2 = 10000$, so that $\mathbf{f}_{c,11}^1 \approx 95\,\text{MHz}$ and $\mathbf{f}_{c,11}^2 \approx 67\,\text{MHz}$.

6.1. Experiment Setup

In our virtual experiments we handle the following representative magnetic profiles:

Table 2. Two arbitrary profiles, in the case of $\mu_c^1 = 5000$, considered "unknown" in the inverse problem (see Figures 5–6).

μ_r^i ($\mu_c^1 = 5000$)
$2850 - 4775.13z + 10241.65z^2 + 20007.53z^3$
$547.5 + 1700.47z - 4350.24z^2 — 2300.92z^3$

Table 3. Three arbitrary profiles, in the case of $\mu_c^1 = 10000$, considered "unknown" in the inverse problem (see Figures 7–9).

μ_r^i ($\mu_c^1 = 10000$)
$47.5 + 1700.11z - 4350.24z^2 - 3000.82z^3$
$350.3 + 3341.27z - 6150.4z^2 - 8400.92z^3$
$187.5 - 200.47z + 1750.24z^2 + 7000.2z^3$

For the genetic algorithm parameters the choices listed in Table 3 yield sufficiently accurate profile estimates.

Also, from various numerical tests we performed, we conclude that $\delta = 10^{-2}$ (three important digits) is a good value for the stopping criterion threshold. This is verified from the figures in Section 6.2 which present the estimated profiles $\widehat{\boldsymbol{\mu}^i}(z)$ in comparison with the real profiles $\mu_r^i(z)$. We obtain these results by using measurements of amplitudes and phases (or real and imaginary parts) of D^i and G^i.

Table 4. G.A.s parameters used in error minimization.

Parameter	Significance
N = 150	Number of trial vectors per generation.
Iterations = 120	Maximum number of generations.
F = 0.5	Diff. Variation amplification.
P = 0.8	Crossover probability.

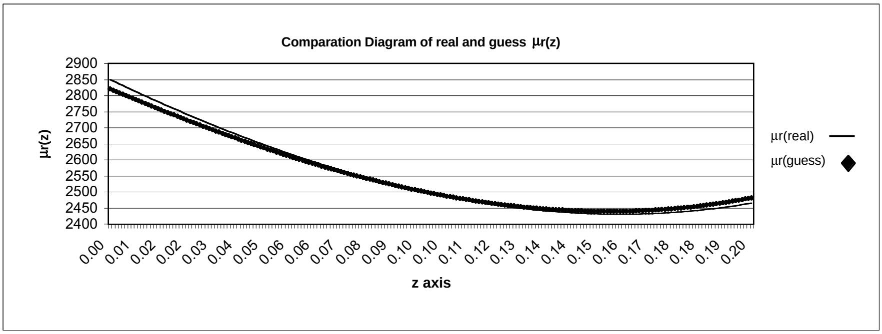

Figure 5. Comparative diagram corresponding to error function value: 0,084. $\mathrm{Max}(|\mu_r(\mathrm{real}) - \mu_r(\mathrm{guess})|) = 29,1$.

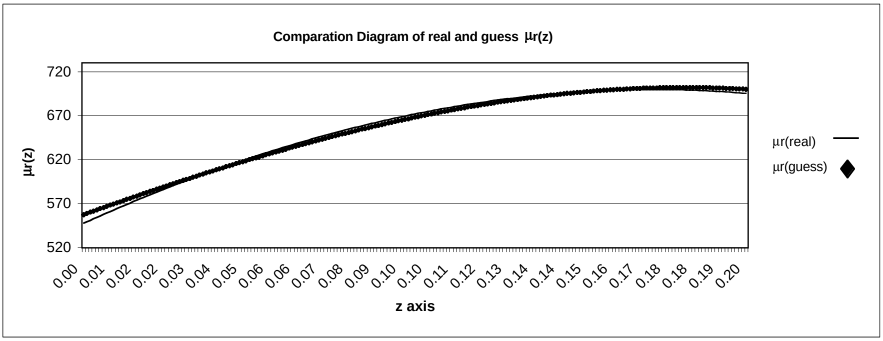

Figure 6. Comparative diagram corresponding to error function value: 0,0313. $\mathrm{Max}(|\mu_r(\mathrm{real}) - \mu_r(\mathrm{guess})|) = 9,81$.

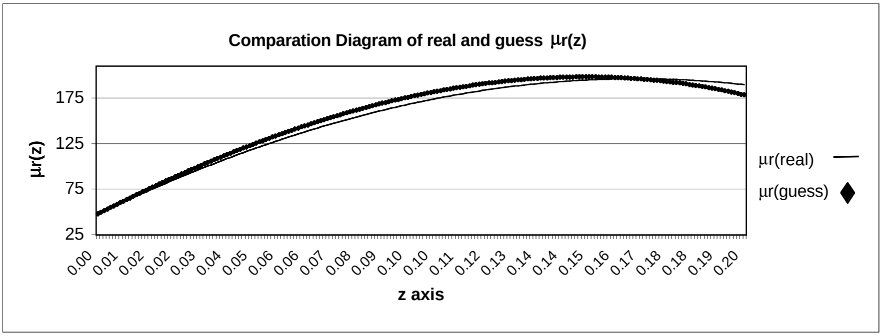

Figure 7. Comparative diagram corresponding to error function value: 0,0313. $\mathrm{Max}(|\mu_r(\mathrm{real}) - \mu_r(\mathrm{guess})|) = 11,12$.

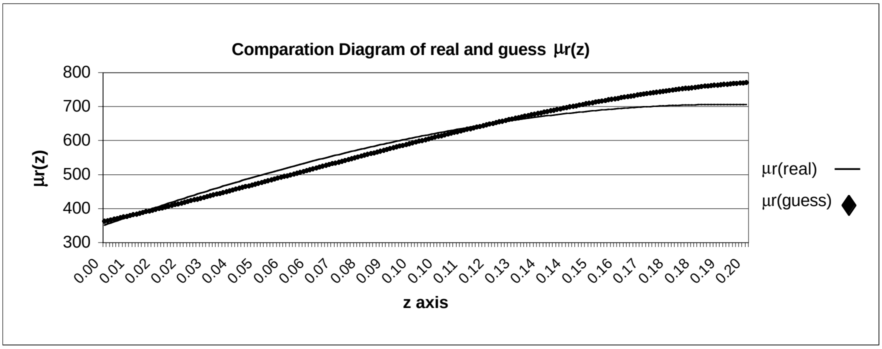

Figure 8. Comparative diagram corresponding to error function value: 0,051. $\mathrm{Max}(|\mu_r(\mathrm{real}) - \mu_r(\mathrm{guess})|) = 64,37$.

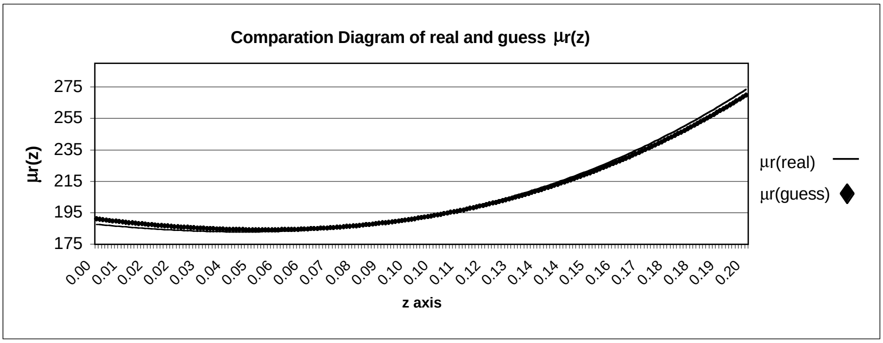

Figure 9. Comparative diagram corresponding to error function value: 0,042. $\mathrm{Max}(|\mu_r(\mathrm{real}) - \mu_r(\mathrm{guess})|) = 3,60$.

6.2. Amplitude & Phase Parts Measurement

The estimates obtained, with respect to the error function value and the threshold δ, give very good approximations for the corresponding magnetic profiles, as can be seen in Figures 5–6 $(\mu_c^1 = 5000)$ and 7–9 $(\mu_c^2 = 10000)$.

7. CONCLUSIONS

In this paper we based on an analytical solution platform to study the wave propagation in an inhomogeneous material in the longitudinal direction. We assumed a simplified theoretical model for an experiment setup and we formulated a direct and an inverse problem as well. The results taken from both were very good and, therefore, this fact adds the strong possibility to reconstruct any unknown inhomogeneous profile expressed as a polynomial of third order. In addition, we used the proposed in [5] technique to estimate the first cut-off frequency of the main propagating mode TM_{11} and we obtained satisfactory results. Thus, it is of question if this technique sustains for waveguides with arbitrary cross section.

REFERENCES

1. Pavlov, D. A. and M. S. Zhdanov, "Anomalous conductivity and magnetic permeability effects in time domain electromagnetic data," *68th Ann. Internat. Mtg., Soc. Expl. Geophys.*, Expanded Abstracts, 440–443, 1998.
2. Pavlov, D. A. and M. S. Zhdanov, "Analysis and interpretation of anomalous conductivity and magnetic permeability effects in time domain electromagnetic, data. Part I: Numerical modeling," *Journal of Applied Geophysics*, Vol. 46, No. 4, 217–233, 2001.
3. Tartaras, E., M. S. Zhdanov, K. Wada, A. Saito, and T. Hara, "Fast imaging of TDEM data based on S-inversion," *Journal of Applied Geophysics*, Vol. 43, No. 1, 15–32, 2000.
4. Cheryauka, A. B. and M. S. Zhdanov, "Nonlinear approximations for an EM scattering problem in a medium with joint electrical and magnetic inhomogeneities," Submitted to *Radio Science.*
5. Baganas, K., A. Charalambopoulos, and A. Kehagias, "Inhomogeneous dielectric media: Wave propagation and dielectric permittivity reconstruction," *SIAM, J. of Electromagn. and Appl.*, Vol. 15, No. 10, 1373–1399, 2001.
6. Baganas, K., "Inhomogeneous dielectric media: Wave propagation and dielectric permittivity reconstruction in the case of a rectangular waveguide," *SIAM, J. of Electromagn. and Appl.*, Vol. 16, No. 10, 1371–1392, 2002.
7. Balanis, K., *Advanced Engineering Electromagnetics*, J. Willey & Sons, N.Y., 1998.
8. Storn, R. and K. Prise, *Differential Evolution — A Simple*

and Efficient Heuristic for Global Optimization over Continuous Spaces, Kluwer Academic Publishers, Vol. 11, 341–359, 1997.

9. Chew, W. C., *Waves and Fields in Inhomogeneous Media*, IEEE Press, 1995.
10. Yashina, N. P., "Reconstruction of various materials' electromagnetic characteristics from the data of wave scattering in a waveguide: analytical regularization," *3rd Intern. ISAAC Congr.*, Berlin, Germany, 2001.

Konstantinos Baganás was born in Greece in 1977. He received the Dipl.-Ing. degree in electrical engineering from the School of Engineering of Aristotle University of Thessaloniki in 2000. He is currently a graduate student at the Department of Materials Science and Engineering of the University of Ioannina and his research interests include electromagnetic, acoustic and elastic wave propagation (direct and inverse problems) in media with inhomogeneities (inclusions, cracks, voids, etc).